Chapter 7

Layers of Inhibitor Anion – Doped Polypyrrole for Corrosion Protection of Mild Steel

Le Minh Duc and Vu Quoc Trung

Additional information is available at the end of the chapter

http://dx.doi.org/10.5772/54573

1. Introduction

1.1. Theoretical background

Almost metals are in contact with wet atmosphere or another aggressive medium such as seawater. Therefore, the corrosion process always occurs on the metal surface. This is also a challenge for scientists to control and reduce the enormous damages due to corrosion. The term ‘corrosion’ refers to deterioration of materials due to the chemical reactions with the environment. Corrosion is involved in the conversion of the surface of metals in contact with corrosive medium into another insoluble compound. Corrosion is also defined as 'the undesirable deterioration' of a metal or an alloy i.e. an interaction of the metal with its environment affecting the main properties of the metal. Corrosion protection is required for a long life and economical use of equipment in technical processes [1, 2].

Corrosion preventing technology has many options, for instance cathodic protection, anodic protection, use of corrosion inhibitors, forming the precipitates on the metal surface and acting as passive layers, organic coatings etc. Among the methods to prevent corrosion of metals, protection by conducting polymers has been investigated extensively in the recent years [3-18]. This is considered as a possible alternative for friendly-environment coating because an electrochemical process could eliminate the use of toxic chemicals. There are many publications related to conducting polymer in corrosion protection. Conducting polymer can decrease the corrosion rate of many metals such as iron, mild steel, aluminium, magnesium and others [19-25].

Conducting polymer has been investigated extensively for corrosion protection of metal. It is observed that a conducting polymer film alone cannot protect an unnoble metal completely. With a galvanic coupling experiment it could be shown that the polymethylthiophene film did

not act as a redox mediator, passivating the steel substrate within the defect and reoxidising itself by dissolved oxygen [26]. Polypyrrole could not provide anodic protection for iron [9, 27]. Conducting polymers like polyaniline, polypyrrole (PPy) etc. can improve the corrosion protection of unnoble metals but it is impossible that the porous films protect the metal surface completely. It is expected that protective properties of polypyrrole can be improved by dopant anion [28].

Counter anions, the so-called dopant anions play an important role in the development of physical properties and morphology. These actions of the anions could be:

- Electroneutralising: dopant anions neutralise the positive charges on the polymer backbone during synthesis of conducting polymers.
- Changing the morphology: the size of the dopant anion can control the microstructure and the porosity of the polymer film.
- Improving the conductivity: the interaction between the positive charges of polymer and anions can influence the conductivity of the polymer films.
- Stabilising the polymer films.
- Compatibility with other polymeric matrices.
- Corrosion inhibition: small dopant anions can be released from the polymer coating when the coating is reduced. If these anions have some inhibiting properties they can provide for some additional protection.

1.2. Mechanism for corrosion protection by polypyrrole

Corrosion at metal surfaces is a severe industrial problem. A large amount of metal is wasted by corrosion. It can cause tremendous economic damages. Minimising this corrosion can save substantial money and prevent accidents due to equipment failure. Corrosion has and continues to be the research object of scientists [1, 2].

Corrosion is an electrochemical process in nature. An anode (negative electrode), a cathode (positive electrode), an electrolyte (environment), and a circuit connecting the anode and the cathode are required for corrosion to occur. For simplicity, the corrosion process of iron in aqueous environment is discussed as a typical example.

The general reaction that occurs at the anode is the dissolution of metal atoms as ions:

$$Fe = Fe^{2+} + 2e$$

Electrons from the anode flow to the cathode area through the metallic circuit and force a cathodic reaction (or reactions) to occur. Depending on the pH of the electrolyte, different cathodic reactions can occur. In alkaline and neutral aerated solutions, the predominant cathodic reaction is

$$O_2 + 2H_2O + 4e \rightarrow 4OH^-$$

In aerated acids, the cathodic reaction could be

http://dx.doi.org/10.5772/54573

$O_2 + 4H^+ + 4e \rightarrow 2H_2O$

In deaerated acids, the cathodic reaction usually occurs is

$2H^+ + 2e \rightarrow H_2$

The corrosion product formed on iron surface in the presence of oxygen is:

$Fe^{2+} + 2OH^- \rightarrow Fe(OH)_2$

This hydrous ferrous oxide ($FeO.nH_2O$) or ferrous oxide $Fe(OH)_2$ composes a diffusion barrier layer on the surface. This layer is green to greenish black in colour. In the presence of oxygen Fe^{2+} is oxidised to Fe^{3+}. Ordinary rust is the product of this step. The formal reaction equation is

$4Fe(OH)_2 + O_2 + 2H_2O = 4Fe(OH)_3$

Hydrous ferric oxide is orange to red-brown in colour. It exists as nonmagnetic Fe_2O_3 (hematite) or as magnetic Fe_2O_3. $Fe_3O_4.nH_2O$ often forms a black intermediate layer between hydrous Fe_2O_3 and FeO. Hence, rust films can consist of up to three layers of iron oxides in different states of oxidation [29].

Beck et al. suggested a model of corrosion protection by PPy [25]. The initial fast corrosion was a superposition of cathodic film reduction and anodic oxidation. Cathodic process was the driving process. The second step was caused of nucleophilic molecules dissolved in the solid. Both processes were of pseudo-first-order.

Jude O. Iroh et al. suggested a corrosion protection mechanism of iron by PPy on the basis of EIS results [10]. The double bonds and the polar –NH group in the ring caused the strong adsorption of PPy and improved corrosion protection. PPy coating was acting as diffusion barrier and was inhibiting charge transfer.

Su and Iroh reported a large shift of the corrosion potential (E_{corr}) nearly 600 mV for PPy(oxalate) on steel compared to bare steel [10]. Reut et al. also recorded this shift of corrosion potential. The different shifts of E_{corr} could be explained by the different pretreatment of the substrate [30]. It was concluded from these results that PPy produced the significant ennobling of steel.

But controversial results were published by Krstajic et al. [9]. It was found that PPy(oxalate) did not provide anodic protection of mild steel in 0.1 M H_2SO_4. PPy was undoped in a short time. The dissolution of the steel continued in the pores of the coating. The mechanism of corrosion protection of steel by PPy is not yet fully understood and it is likely to change with the corrosion conditions [30].

PPy film doped with inhibitor anions such as molybdate were synthesised on mild steel in a one-step process. Corrosion tests indicated a significant improvement of the protective performance of PPy film. PPy coatings even prevented corrosion in defect of the coating. Now the corrosion protection mechanism of PPy with small defect on mild steel will be discussed.

A defect on PPy coating deposited on mild steel substrate may be produced either because of manufacturing or due to damage. When this occurs, bare mild steel is exposed to the corrosive atmosphere. The oxidation of substrate occurs. The following corrosion or anodic reaction takes place at the bottom of the defect:

$$Fe = Fe^{2+} + 2e \quad (1)$$

The open circuit potential of the coated sample drops down to the corrosion potential of iron if the sample is immersed in NaCl (see Figure 11).

The electrons produced in (1) are consumed in cathodic reactions as followed:

$$O_2 + 2H_2O + 4e = 4OH^- \quad (2)$$

$$PPy_{OX}(DOP) + ne = PPy_{RED} + DOP^{n-} \quad (3)$$

Where PPy_{OX}, PPy_{RED} are the oxidised and reduced states of polypyrrole, respectively. DOP^{n-} is a dopant anion.

The PPy film is reduced (reaction 3) as a result of the galvanically coupling to metal substrate. Reaction (2) takes place within the defect as well as on PPy film if Ppy is conductive and can mediate the electron transfer [31, 32].

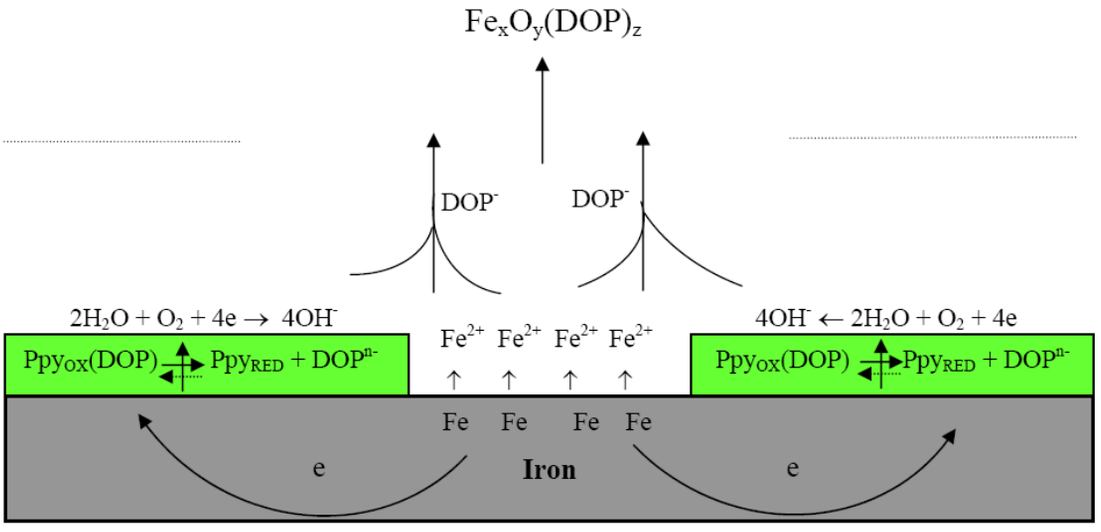

Figure 1. Model for the mechanism of corrosion protection of PPy proposed by Plieth et al. [34-36].

The dopant anions DOP^{n-} form insoluble salts or complexes $[Fe_xO_y(DOP)]$ with iron ions and can prevent further corrosion. In other words, the defect is repaired by the inhibitor anions produced during the reduction of PPy film.

Based on the model of Kinlen [33], the proposed mechanism of corrosion protection of PPy is developed as in figure 1 [34-36]. However, from the results of the OCP and EIS measurement re-oxidation of conducting polymer by of oxygen could not be found.

http://dx.doi.org/10.5772/54573

In most studies on the corrosion protection of mild steel by PPy, the role of the dopant anion as corrosion inhibitor has been investigated somewhere. The use of large anions such as polystyrensulfonate, dodecyl sulphate could improve the corrosion protection of the PPy film by preventing the penetration of chloride [20, 21]. Corrosion is not inhibited if the coating has small defects. The defect is protected only if inhibitor anions can diffuse to the defect. Thus, the mobility of dopant anions is one of the important parameters. The release of dopant anions from the polypyrrole film is the first step of corrosion inhibition. Further studies presented in this chapter are necessary to understand the role of dopants in PPy film for corrosion protection. In addition, the organic coatings (such as epoxy) containing nanocomposites based on suitable anion doped PPy seems to be an useful solution for application to replace the toxic cromate paitings. Therrefore, in this chapter the corrosion protection of mild steel of epoxy coatings using doped PPy nanocomposites is also presented.

2. Experimental and analytical methods

2.1. Chemicals

Pyrrole monomers (Aldrich, 98-99%), $LiClO_4$ (Fluka, P.A), $(C_4H_9)_4NBr$ (Merck, P.A), Na_2MoO_4 (Aldrich), Na_2MoO_4 (Acros) and NaCl (J.T.Baker, P.A). Clay obtained from Di Linh mine, Vietnam, was refined by suspension method and then was sodized. Epoxy resin was received from Dow (D.E.R 324); hardener DETA (Diethylentriamin) was also perchased from Dow (USA) with amount of 10%.

2.2. Equipment

The following equipment was employed:

* EG&G-263A Model potentiostat/galvanostat.

* IM6 and Zenium impedance measurement system of ZAHNER-Elektrik. The ZAHNER simulation software was integrated in this system. The frequency range used was 100 kHz – 0.1 Hz.

* The network analyser Advantest R3753BH was connected to the EG&G-263A Model potentiostat/galvanostat to measure the impedance of the quartz electrode in EQCM.

* SEM pictures were obtained with Zeiss DSM 982 Gemini microscope (Carl Zeiss, Germany).

* Raman Spectrometer Series 1000 – Renishaw.

2.3. Cell of measurements

2.3.1. Cell for electropolymerisation

The cell consisted of two parts which can be screwed together by Teflon screws. The working electrode (WE) was placed between of them. A silicon ring was used for sealing. The surface

of the WE was 0.64 cm^2. The Pt sheet counter electrode (CE) was placed in a narrow slot. The distance between anode and cathode was 2.5 cm. The reference electrode was connected with the working electrode through a salt bridge.

2.3.2. Cell for EIS measurement

The EIS cell consisted of two parts which could be fixed to each other with four metal screws at the corners. The working electrode was placed between these parts. A silicon gasket defined the immersion surface of working electrode (0.125 cm^2). A glass container was placed on the upper part to hold the electrolyte. Pt net was the counter electrode.

2.4. Pretreatments of substrates

The substrates were pretreated as below:

- Mild steel (20 x 20 mm^2): Polishing with emery paper No 600; rinsing in ethanol in an ultrasonic bath for about 15 minutes; then drying in an N_2 stream.
- Passive film on mild steel (20 x 20 mm^2): Treating as described above; immersion in 0.1 M Na_2MoO_4 for 60 minutes, 30^0C; potentiostatic passivation at 0.5 V_{SCE} for 1 hour; rinsing in distilled water and drying in an N_2 stream.

2.5. Condition for electrochemical polymerisation of polypyrrole

The PPy films were generated galvanostatically on the pretreated mild steel surface at a current density of 1.5 $mA.cm^{-2}$ in an aqueous solution of 0.1 M pyrrole (from Aldrich 98%, keep at 4^oC and distil in argon atmosphere before using) and 0.01 M sodium molybdate (pH=4.8). After forming, the sample was rinsed in distilled water and dried in nitrogen atmosphere. The film thickness was about 1–1.2 μm. For investigation of the release behaviour of molybdate anion during the reduction of PPy, the films were electrodeposited on Pt.

2.6. Condition for chemical preparation of molybdate anions doped polypyrrole/ montmorillonite nanocomposites PPy(MoO_4)/MMT

Nanomposites were prepared following a procedure described in Ref. [37, 38]. Firstly, a dispersion was prepared by mixing (for 30 min.) of 3.0 g Na^+-MMT, 0.87 g dopant and 1.0 mL pyrrole monomers in distilled water. Then 3.94 g $(NH_4)_2S_2O_8$ was added to the dispersion during stirring. The colour of the mixture was changed from grey to black. After 2 hours of stirring, the solid product was cleaned by distilled water, filtered and dried at 40-50^0C for 6 hours under low pressure.

2.7. Preparation of epoxy coatings

Epoxy coatings containing molybdate anions doped PPy/montmorillonite nanocomposites PPy(MoO_4)/MMT were prepared by spray. The thickness of the coatings are 50-60μm. The amounts of PPy(MoO_4)/MMT in the coatings are 2; 3; 4% (by weight).

http://dx.doi.org/10.5772/54573

2.8. Electrochemical impedance spectroscopy and its interpretation

Electrochemical Impedance Spectroscopy (EIS) primarily characterises a conducting polymer system in terms of electrical properties. The electrochemical behaviour of the polymer film is substituted by an equivalent circuit. The typical Bode plot and the equivalent circuit of a Ppy film are shown in Figure 2 and in Figure 3, respectively.

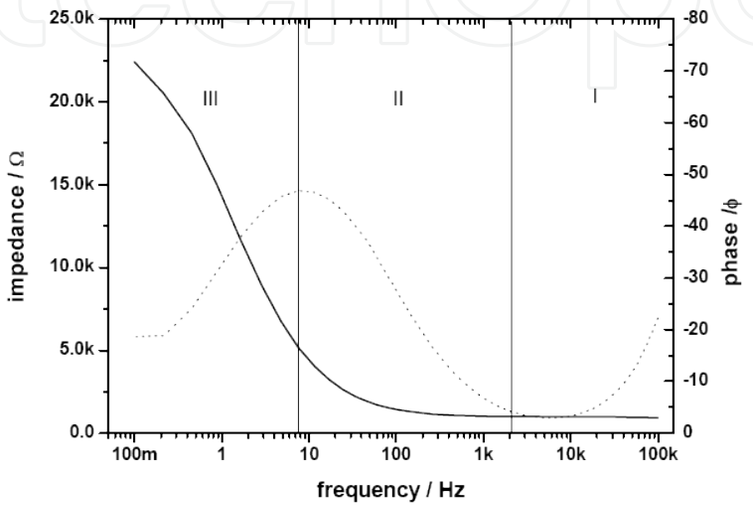

Figure 2. Bode of PPy film: Impedance (solid line) and phase angle (dot line)

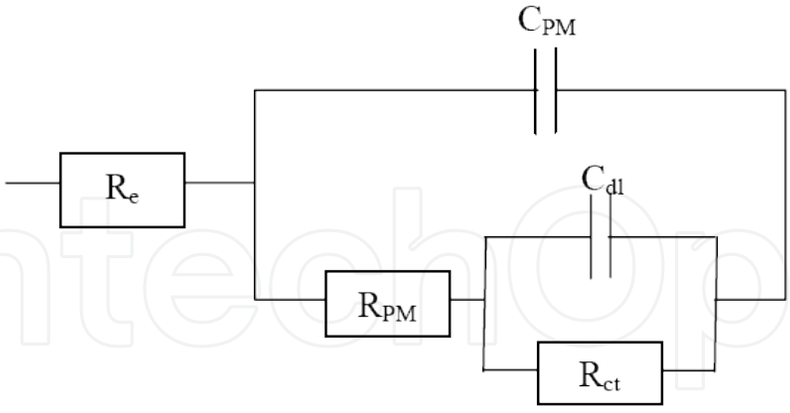

Figure 3. Equivalent circuit for fitting the impedance spectrum of PPy films [34-36].

The obtained impedance spectra of the polymer film can be divided in three regions:

- Region I (*high frequency > 1 kHz*): characterises the behaviour of the electrolyte. Phase angle is nearly zero (dotted line in Figure 2). The resistance of the electrolyte is described by Re in the equivalent circuit (Figure 3).

- Region II (*middle frequency*): shows the properties of the polymer film. The PPy film behaves as dielectricum with a capacitive impedance. The behaviour is simulated by a capacitance C_{PM} parallel to the resistance of the polymer film R_{PM}.
- Region III (*low frequency*): represents the interface polymer/substrate. C_{dl} and R_{ct} are the capacitance of double layer and the charge transfer resistance of the interface, respectively.

The experimental EIS data could be modelled by the equivalent circuit in Figure 3 using the fitting procedure of Zahner software.

3. Results and discussions

3.1. Molybdate anions doped polypyrrole films for corrosion protection

3.1.1. Electropolymerisation of pyrrole on mild steel

Electrochemical polymerisation of pyrrole on metals such as Fe, Zn, Al, and Mg is prevented by the oxidation of these metals because the oxidation potentials are lower than that of pyrrole. The dissolution of metals is so large that the PPy film has no adhesion to the substrate. This problem can be overcome by many methods [39], one of them is the proper selection of the electrolyte.

The role of molybdate as an inhibitor stored in the PPy film as well as the use of the PPy to protect mild steel from corrosion is discussed in the part of theoretical background.

3.1.2. Behaviour of mild steel in molybdate solution

Figure 4 shows the open circuit potential (OCP) vs. time curves of the mild steel electrode immersed in aerated and deaerated aqueous solution of 0.01 M Na_2MoO_4.

As seen in Figure 4, in both cases, the OCP shifts rapidly to positive potentials towards the passive region of mild steel. This potential rise can be ascribed to the reaction between molybdate anions and mild steel as soon as the electrode is immersed into the solution. The insoluble product can block the surface and make the surface potential more positive. This effect can be seen in deaerated medium. In the presence of oxygen, however, the OCP shift is faster and achieves larger positive potentials.

In other words, MoO_4^{2-} compound acts as an oxidant and passivates the surface of mild steel surface shortly even if without oxygen. Surface analysis of mild steel exposed to molybdate by XPS, AES and an electron microprobe confirms the presence of FeO.OH in combination with MoO_3 [40]. In contrast, the passivation of mild steel needs oxygen in solutions containing inhibitor such as oxalate, succinate, and phthalate [41].

http://dx.doi.org/10.5772/54573

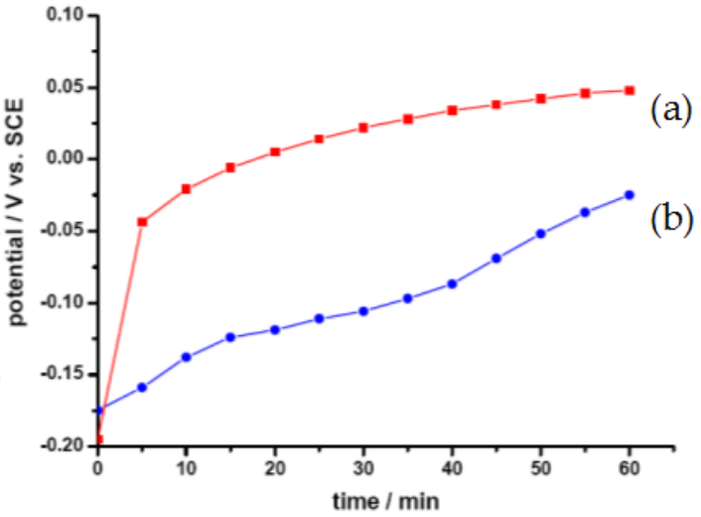

Figure 4. OCP – time curve of mild steel in aerated (a) and in deaerated (b) 0.01 M Na_2MoO_4

3.1.3. Electropolymerisation of pyrrole on mild steel

The PPy films were generated galvanostatically at a current density of 1.5 mA cm^{-2} in an aqueous solution of 0.1 M pyrrole and 0.01M sodium molybdate (pH=4.8). The total charge passed was 0.9 C cm^{-2}.

After formation, the sample was rinsed in distilled water and dried in nitrogen atmosphere. The potential-time curve for galvanic deposition of PPy(MoO_4) on mild steel is shown in Figure 5.

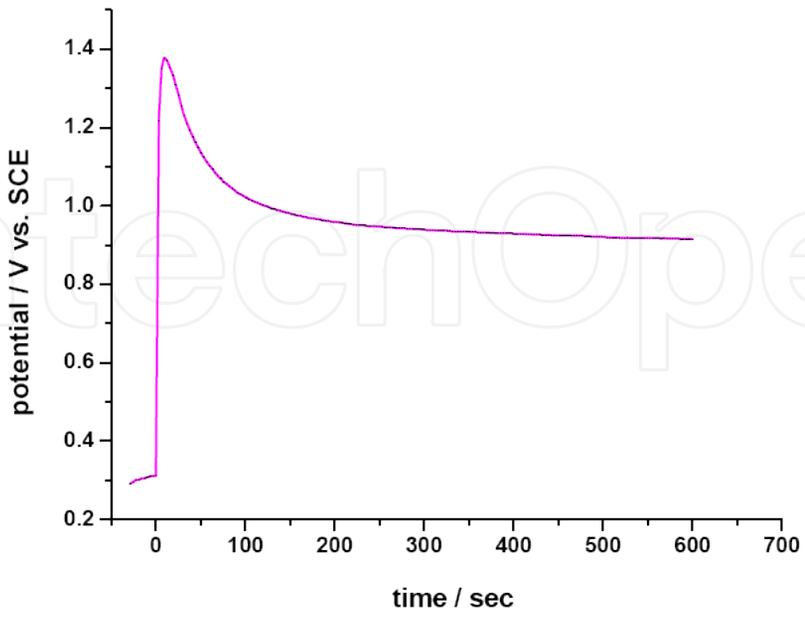

Figure 5. Electrochemical polymerization of pyrrole on mild steel (i = 1.5 mA.cm^{-2}; 0.01 M MoO_4^{2-}; pH = 4.8; 0.1 M pyrrole)

The polymerisation starts at a constant current of 1.5 mA.cm^{-2} for which the potential increases rapidly and then decreases slowly. After 100 seconds, the potential is stabilised at about 0.9 V_{SCE} which corresponds to the oxidation potential of pyrrole.

This behaviour indicates that the dissolution of mild steel is prevented. Pyrrole can be oxidised on mild steel. However, the oxidation potential of pyrrole is higher than normal. The reasons may be: i) the barrier effect of the passivating layer of molybdate on the surface ii) the lower conductivity of the electrolyte.

It should be noted that the polymerisation in presence of molybdate on mild steel occurs without an induction period. This is in contrast to other procedures which have been reported [20, 42, 43]. The electropolymerisation of pyrrole in oxalate aqueous solution is a typical example to elucidate the role of molybdate in the polymerisation. An induction time is present during the polymerisation as shown in Figure 6.

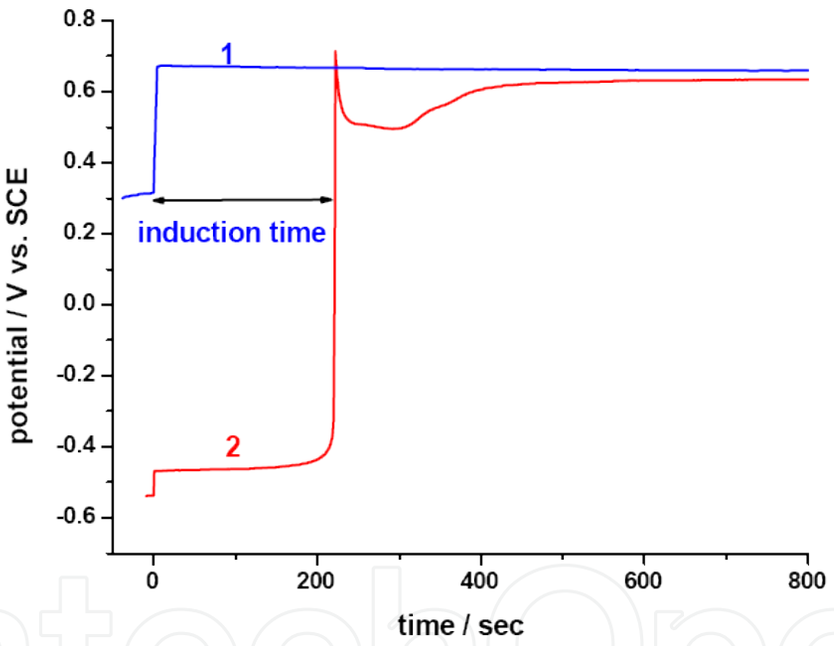

Figure 6. Potential – time curve for the electrodeposition of PPy on Pt(1) and on mild steel (2) from 0.1 M $H_2C_2O_4$; 0.1 M pyrrole, at 1 mA.cm^{-2}

Obviously, the surface of mild steel needs nearly 200 seconds to be passivated in oxalic acid ($H_2C_2O_4$). The induction time is attributed to the active dissolution of mild steel. This active range is assigned at the negative potential. Next, the formation of Fe-oxalate results in the potential shift towards positive potentials high enough for oxidation of pyrrole. Finally, the positive potential levels off until the end of polymerisation. The behaviour is different from that of the electropolymerisation on Pt. Pyrrole can be oxidised immediately on Pt after applying the current through the cell.

3.1.4. Characterisation of PPy(MoO_4)/mild steel film

3.1.4.1. Film morphology

Figure 7 shows SEM micrographs of PPy films doped with MoO_4^{2-} on mild steel (left) and on Pt (right). The total consumed charge for deposition was about 0.9 C cm^{-2}. The films formed on mild steel are homogenous, compact, but thinner than on Pt. The typical cauliflower structure of PPy films on mild steel is observed.

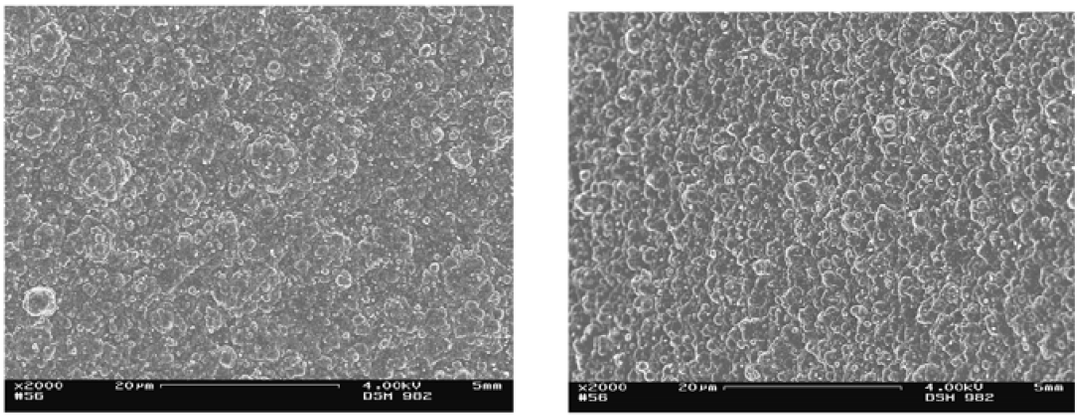

Figure 7. SEM pictures of PPy(MoO_4) on mild steel (left) and on Pt (right)

3.1.4.2. Thickness of PPy films on mild steel

A PPy film was formed on mild steel at the condition mentioned above, and then covered by conducting resin. A cross-section of the sample was made by cutting and polishing with 1200 emery paper. SEM and Energy Dispersive X-ray (EDX) measurements were carried out to determine the thickness of the PPy film.

As seen in Figure 8, three parts can be distinguished clearly. The Ppy film is determined in the middle part. The thickness of the Ppy film was estimated to about 1.2 µm, the charge consumed was 0.9 C cm^{-2}. The result is reproducible.

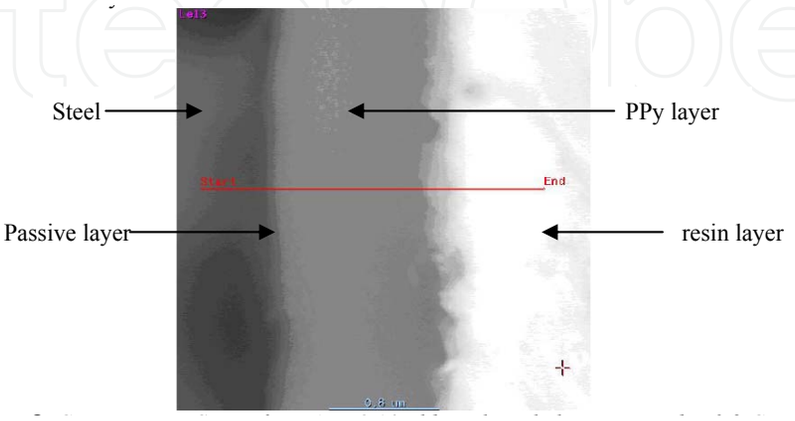

Figure 8. Figure 8. Cross-section SEM of PPy(MoO_4)/mild steel total charge passed is 0.9 C.cm^{-2}

It has been known that total charge for electropolymerisation of pyrrole is about 0.4 C $cm^{-2}\mu^{-1}$ on inert electrodes such as platinum. The value obtained in the current experiment is 0.75 C $\mu^{-1}cm^{-2}$. The reason of this difference may be: a part of charge is used for the passivation of mild steel with molybdate.

3.1.4.3. XPS analysis

XPS spectra for molybdate in PPy(MoO_4) on mild steel presented in [44] showed the XPS surface analysis of the PPy(MoO_4) on mild steel. PPy was electrodeposited under similar conditions mentioned above.

The complex spectra of Mo 3d peaks correspond to the chemical states. The peaks are assigned: $Mo1_{3d5}$ (231 eV), $Mo1_{3d3}$ (233 eV), $Mo2_{3d5}$ (234.5 eV) and $Mo2_{3d3}$ (236 eV) [45]. The XPS spectra are supposed that molybdate should be in two compounds: $[MoO_4]^{2-}$ (62%) and $[Mo_7O_{24}]^{6-}$ (38%). Both types of molybdate are doped in PPy.

One should take into account the fact that molybdate exist in different forms depending on the pH of solution [46]. This relation can be presented:

$$[MoO_4]^{2-} \Leftrightarrow [Mo_7O_{24}]^{6-} \Leftrightarrow [Mo_8O_{26}]^{4-} \Leftrightarrow [Mo_{36}O_{112}]^{8-} \Leftrightarrow MoO_3 \cdot 2H_2O$$

pH=6.5 – 4.5 pH=2.9 pH<2 pH= 0.9

In this condition of electropolymerisation (pH about 4.8), the presence of $[MoO_4]^{2-}$ and $[Mo_7O_{24}]^{6-}$ in polymer film is obvious.

3.1.5. Anion release from Ppy(MoO_4)/mild steel

Electrochemical behaviour of PPy on mild steel was characterised by EIS combined with cyclic voltammetry. Figure 9 shows the change of the resistance R_{PM} and the capacitance C_{PM} of PPy(MoO_4)/mild steel with the potential.

In the potential range from 0.6 V - 0.2 V_{SCE}, the PPy film is conductive; R_{PM} is small (about 20 Ω). Following the negative scan, R_{PM} increases gradually. The reduction of the PPy film begins at 0.2 V_{SCE}. The behaviour is reversible (see reverse scan) i.e. R_{PM} decreases nearly to the original value. The PPy(MoO_4) film is now in the oxidised state.

The change of the film capacitance C_{PM} is inversely proportional to that of R_{PM}. It decreases in the negative scan and increases in the positive scan gradually. It is observed, however, that the film capacitance does not return to the original value. The explanation for this phenomenon is that the transport of solvent (water) accompanies by the anion exchange. It leads to the conformation changes of the conducting polymer.

Hence, it can be concluded that:

- PPy(MoO_4) can be synthesised electrochemically on active metals like mild steel, in a one-step process. The dissolution of mild steel can be prevented with molybdate. The film is homogenous and adhesive on mild steel.

http://dx.doi.org/10.5772/54573

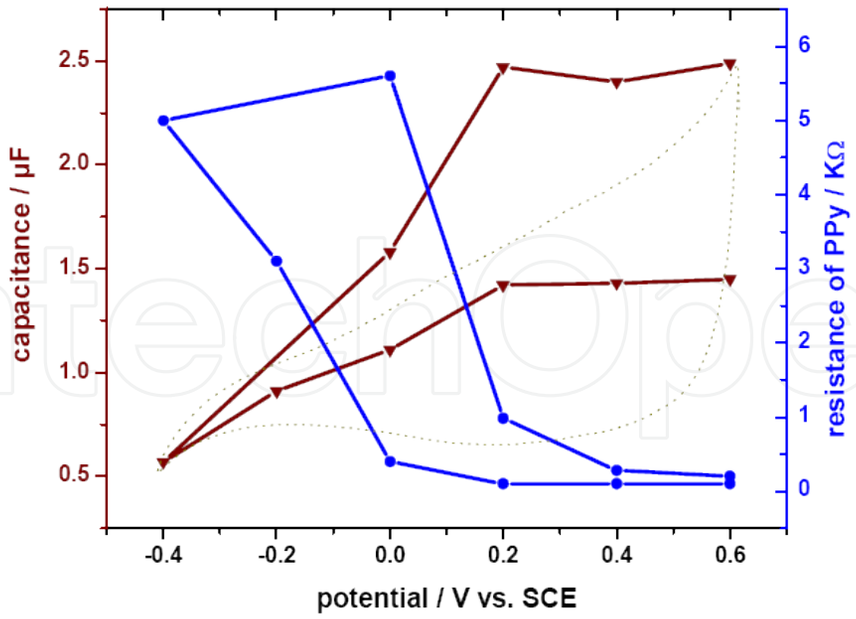

Figure 9. Change of R_{PM} and C_{PM} during reduction of PPy(MoO_4)/mild steel in 0.1 M $(Bu)_4NBr$, N_2, Dotted line is the CV

- PPy(MoO_4) film formed on mild steel has the same redox property as on Pt. During reduction in $(Bu)_4NBr$ solution the decrease of film capacitance is observed. It means that molybdate releases from the film.
- There is no evidence of film decomposition. Corrosion test of PPy(MoO_4) on mild steel

3.1.6. Polarisation curves

The protective effect of PPy(MoO_4) film on mild steel was examined in aerated 0.1 M NaCl. The corrosion potential E_{corr} and corrosion current density i_{corr} was determined by extrapolation of anodic and cathodic Tafel lines.

Figure 10 indicates that E_{corr} shifts towards positive potentials (about 500 mV) and i_{corr} decreases about one order in magnitude as compared to the bare mild steel electrode. The polymer film can prevent the metal surface from corrosion. The inhibiting efficiency E of PPy(MoO_4) is obtained by equation:

$$E = \frac{i^o - i}{i^o}\%$$

Where i^o, i denote the corrosion current of bare mild steel and PPy(MoO_4)/mild steel, respectively. The inhibiting efficiency E is about 98% for PPy(MoO_4) on mild steel.

3.1.7. OCP measurement

The corrosion behaviour of mild steel covered by PPy(MoO_4) films was investigated by OCP-time measurements. The samples were immersed in a 0.1 M NaCl solution as corrosive medium and the OCP was recorded versus time. The protection time is characterised by the

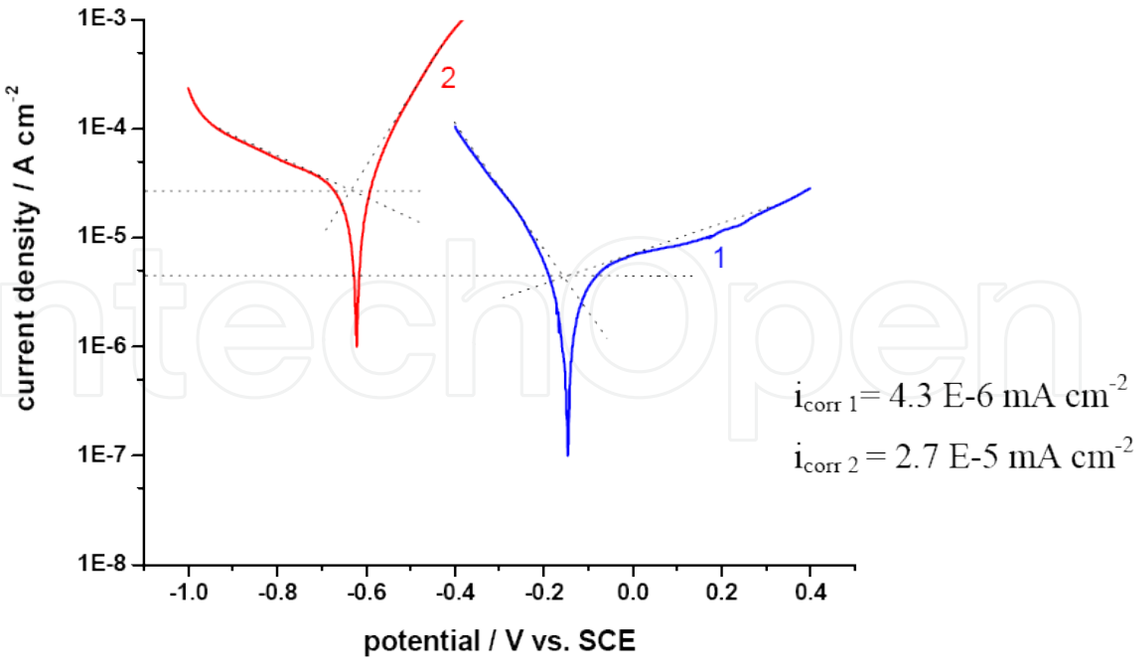

Figure 10. Potentiodynamic curve of PPy(MoO_4)/mild steel film (1) and bare mild steel (2) in 0.1 M NaCl, 1 mV.s^{-1}

time during which the OCP of the covered electrode remains in the passive state of mild steel before it drops down to the corrosion potential of unprotected mild steel.

The OCP-time curve of PPy(MoO_4) coated on mild steel in NaCl is presented in Figure 11. The OCP is initially positive at about 0.35 V_{SCE} which corresponds to redox potential of PPy. The mild steel electrode maintains in its passive state for about 7 hours. Then, the potential sharply decreases to a second plateau at about -0.2 V_{SCE} and is stable there for about 5 hours. In this plateau, chloride anions have reached the metal surface through the pores of PPy film. The anodic reaction can take place and the polymer is reduced partially. This reduction causes the molybdate anion release which is needed to slow down the corrosion rate. This may be a reason why OCP is stable at plateau 2. The release of molybdate from the PPy film in this second plateau was confirmed by EIS measurement shown in Figure 12. The reduction of PPy film causes the increase of the film resistance (marked by an arrow) and the release of molybdate causes the decrease of the film capacitance.

Finally, OCP decreases towards the corrosion potential of the mild steel because of the large concentration of chloride in the polymer/mild steel interface, PPy cannot protect mild steel any longer.

This second plateau is only observed if the dopant anions of the conducting polymer have some ability to inhibit the corrosion reaction of mild steel [9, 20]. If the anions cannot give this protection, the second plateau is missing and the potential falls down to the corrosion potential of mild steel at the end of the first plateau [47].

PPy(MoO_4) has shown the protective ability for mild steel. The corrosion potential is kept at the second plateau where mild steel is in a passive state.

http://dx.doi.org/10.5772/54573

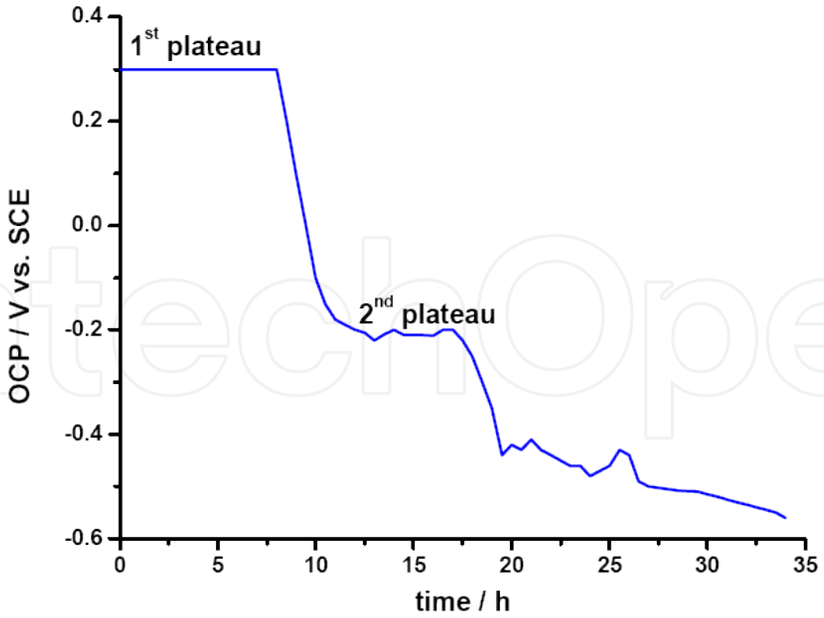

Figure 11. OCP-time curve of PPy(MoO_4)/mild steel (thickness of 1.5 µm) in 0.1 M NaCl

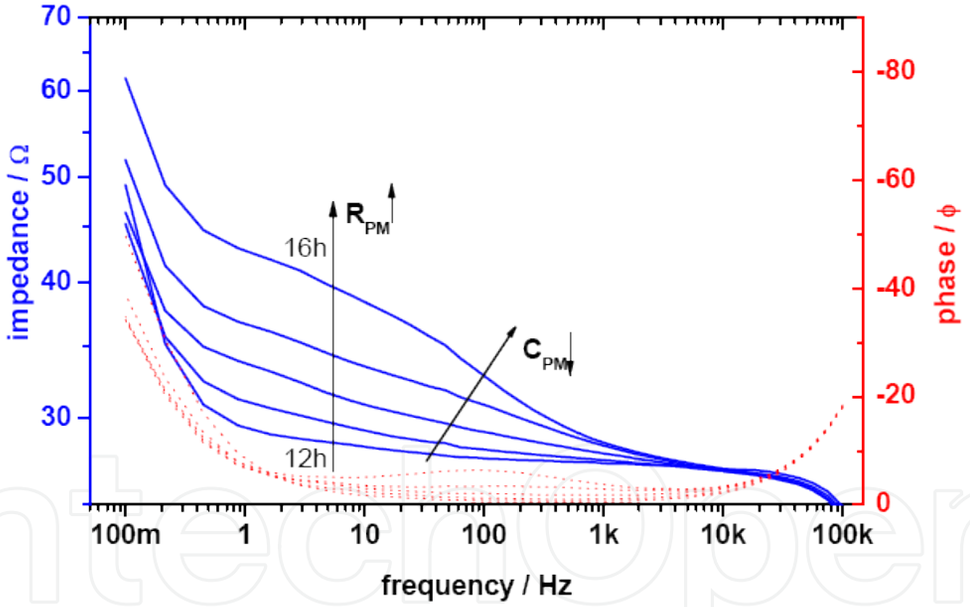

Figure 12. EIS spectra of the PPy(MoO4) film in the second plateau of the OCP in 0.1 M NaCl solution. Impedance (solid line) and phase angle (dotted line)

3.1.8. The role of molybdate passive layers in corrosion protection

It is clear that a passive layer of molybdate is formed on mild steel during the electropolymerisation process. This layer can reduce the oxidation of mild steel and facilitates the polymerisation of pyrrole. In order to clarify the role of molybdate in this passive layer in corrosion protection, a PPy film with the non-inhibitive anions ClO_4^- was electrodeposited on

mild steel passivated with molybdate. The corrosion test was carried out in 0.1 M NaCl solution.

A mild steel electrode was passivated in molybdate solution with the following procedure: immersion in 0.1 M Na_2MoO_4 for 60 minutes, 30°C; potentiostatic passivation at 0.5 V_{SCE} for 1 hour; rinsing in distilled water and drying under N_2 stream [48]. The PPy(ClO_4) film was electrodeposited under these conditions: 0.1 M $LiClO_4$, 0.1 M pyrrole monomer, i = 1 mA cm^{-2}. The OCP of PPy(ClO_4) was recorded in 0.1 M NaCl.

Figure 13 shows the OCP-time curve of PPy(ClO_4)/passive layer/mild steel in 0.1 M NaCl. At the beginning, the OCP is still in the passive range of mild steel. PPy(ClO_4) can protect the substrate from corrosion. Nevertheless, this protection only remains for a short time (about 100 seconds). The penetration of chloride through the film is very fast and breaks down the passive film of molybdate formed in the pretreatment procedure. The OCP decreases sharply to the active potential range.

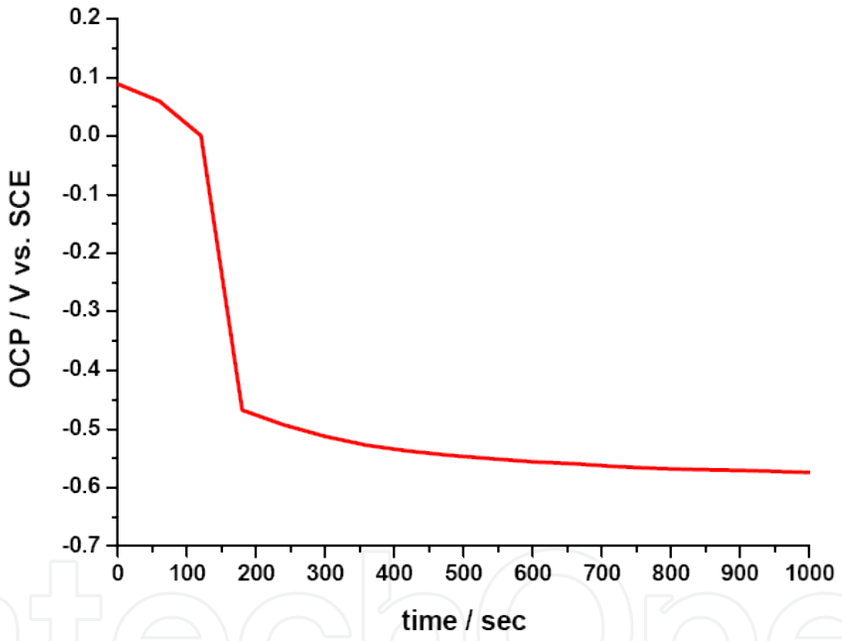

Figure 13. OCP-time vurve of PPy(ClO_4)/passive layer/mild steel in 0.1 M NaCl

This OCP measurement indicates that the passive film of molybdate on the mild steel cannot prevent the penetration of chloride and cannot reduce the corrosion rate. Molybdate in a passive layer under the polymer film does not play any role for corrosion protection.

3.1.9. The possibility of self-healing with PPy(MoO_4) film on mild steel

The self-healing action of PPy(MoO_4) film was investigated. On a fresh PPy(MoO_4)/mild steel film, a small defect (about 0.04 mm^2) was made with a needle. OCP–time curve was recorded in aerated 0.1 M NaCl as seen in Figure 14.

http://dx.doi.org/10.5772/54573

After immersion, the potential decreases immediately and then levels off at a potential of about -0.1 V for 4 hours. This observation could be explained as follows: the dissolution of mild steel at defect occurs immediately after the PPy film contacts with the corrosive environment. Because of the galvanical connection with mild steel, PPy will be reduced to compensate the redox process. This reduction is a driving-force for molybdate anions to be released from the PPy near the defect. A passive compound $Fe_xMo_yO_z$ is produced and it acts as inhibitor in the defect. It results in the maintenance of the potential for a certain time. The fluctuation of the OCP, numerous small spikes of potential are observed, is explained as the breakdown of the passive film by chloride and the re-passivation by MoO_4^{2-} in the defects. A small defect of the PPy film is protected from corrosion by the PPy(MoO_4) film.

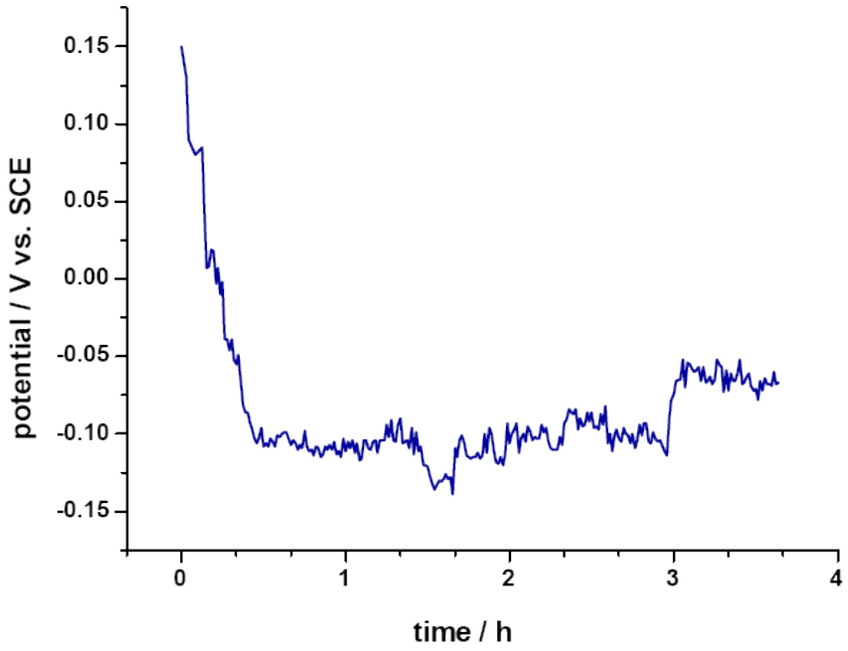

Figure 14. OCP of PPy(MoO_4)/mild steel with a defect (about 0.04 mm^2) *in aerated 0.1 M NaCl*

The same experiment was carried out with a PPy film doped with PF_6^- as non-inhibitive anion. After passivating with molybdate, a mild steel electrode was covered with PPy in 0.1 M $(Bu)_4NPF_6$, 0.1 M pyrrole in dichloromethane at 1.5 mA cm^{-2}. A small defect was made with a needle (0.04 mm^2) on the fresh film. As corrosive medium 0.1 M NaCl was also used.

The polarisation curves shown in Figure 15 are obtained on two PPy films with different dopant anions, namely PF_6^- (curve 1) and molybdate (curve 2). Although there is a molybdate passive layer, the corrosion potential of PPy(PF_6) is still in the active range at the beginning of the experiment. No shift of the corrosion potential is observed here. This behaviour shows that the defect is attacked continuously by chloride. PPy(PF_6) film cannot protect and repair this defect.

On the contrary, a positive shift of the corrosion potential and the decrease of the corrosion current are observed on PPy(MoO_4)/mild steel (curve 2). The defect is passivated for 4 hours.

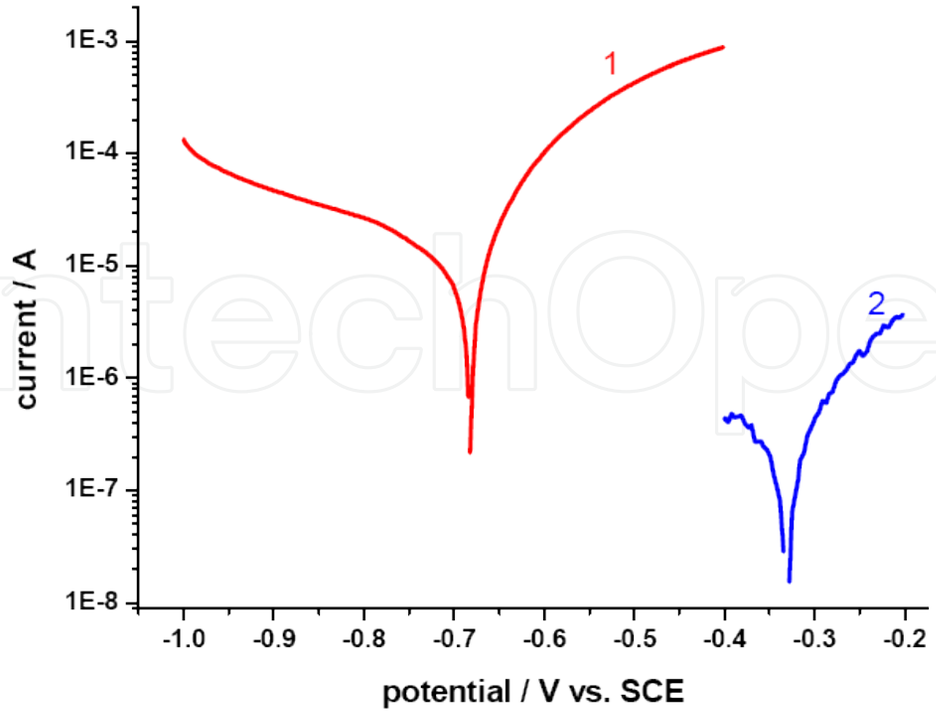

Figure 15. Fe/molybdate passive layer/PPy (PF_6), i=1.5 mA.cm^{-2}, in dichloromethane, about 1.5 µm; (2): Fe/PPy(MoO_4), ca. 1.5 µm, after dipping 4 hours

The corrosion potential remains in the passive range. The corrosion current for PPy(MoO_4) is nearly two orders of magnitude smaller than that of PPy(PF_6).

These results show that molybdate within a polymer plays an important role in self-healing of a defect. Passive layers containing molybdate on mild steel can reduce the dissolution of the active metal during the polymerisation but cannot act as corrosion inhibitor. The self-healing action for mild steel only takes place on PPy films doped with corrosion inhibitors such as molybdate.

3.1.10. Delamination

The corrosion process of PPy(MoO_4) on mild steel was investigated with the Scanning Kelvinprobe (SKP). The experimental set-up and the SKP measurements were made in MPI (Max-Planck Institute for Iron, Dusseldorf - Germany). The artificial defect was prepared on a part of PPy film shown in Figure 16.

The used SKP tip had a diameter of 100µm. Top-coat was polyacryl resin (BASF) applied on the film in order to avoid the difficulties resulting from the folding of the film during the delamination experiment. The humid atmosphere (93 – 95%) was controlled during the experiment.

PPy was formed on mild steel under the following conditions: 0.1 M pyrrole + 0.01 M molybdate aqueous electrolyte; current density 1.5 mA cm^{-2}. The SKP measurements were obtained in 0.1 M KCl solution. SKP experiment of PPy(MoO4)/mild steel in 0.1 M KCl presented in [34]

http://dx.doi.org/10.5772/54573

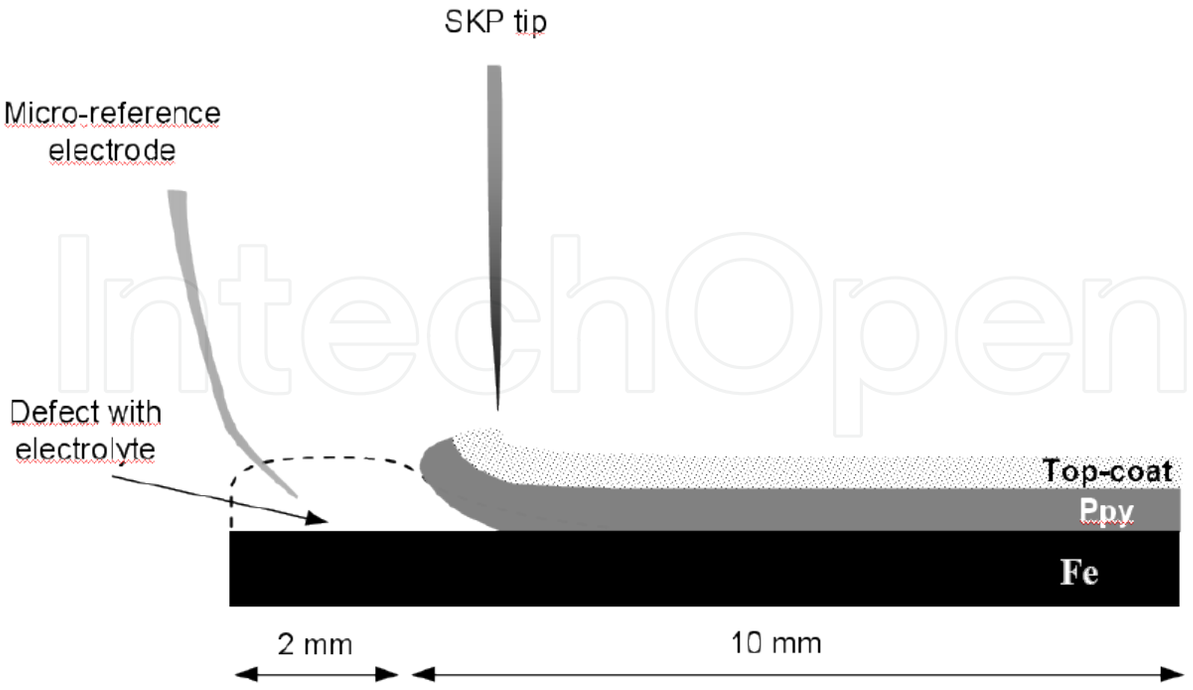

Figure 16. Preparation of iron electrode coated by PPy(MoO_4) folm for SKP experiment [34]

showed the profile of corrosion potential E_{corr} as function of the distance defect border for different times after contact of the defect with electrolyte. The features must be mentioned: (i) the region next to the defect where E_{corr} is similar corrosion potential of bare mild steel (-0.45 V_{SHE}). (ii) a region of abrupt increase low to high values of E_{corr}. This region shifts from left to right i.e. away from border with increasing time; (iii) a region where the adhesion is not yet lost [49].

It can be seen that the delamination of PPy film is very fast in KCl (about 1600 μm for 2 hours). The corrosion potential of the delaminated area remains in the active range potential of corroding iron (about 0.45 V_{SHE}). The passivation of the defect does not take place.

Because of their size, cations K^+ can move into the PPy film easier than the release of molybdate from the film during delamination process. The transport of anions in electrochemical experiment is only few micron while the delamination over hundreds micron, that leads to the predominately cation incorporation into the film for charge compensation. The amount of molybdate is not enough to passivate the large defect.

The delamination of PPy(MoO_4) film on mild steel investigated further in 0.1 M $(Bu)_4NCl$ solution is shown in Figure 17. The delamination is much slower than that in small cation solution. Now the delamination front reaches 1600μm after 33 hours instead of 2 hours in KCl solution. The reduction of PPy at the defect is slowed down. Obviously, the size of cation in electrolyte had effects on the delamination process. The incorporation of cation $N(Bu)_4^+$ is hindered because of their size. The release of molybdate anions is predominant.

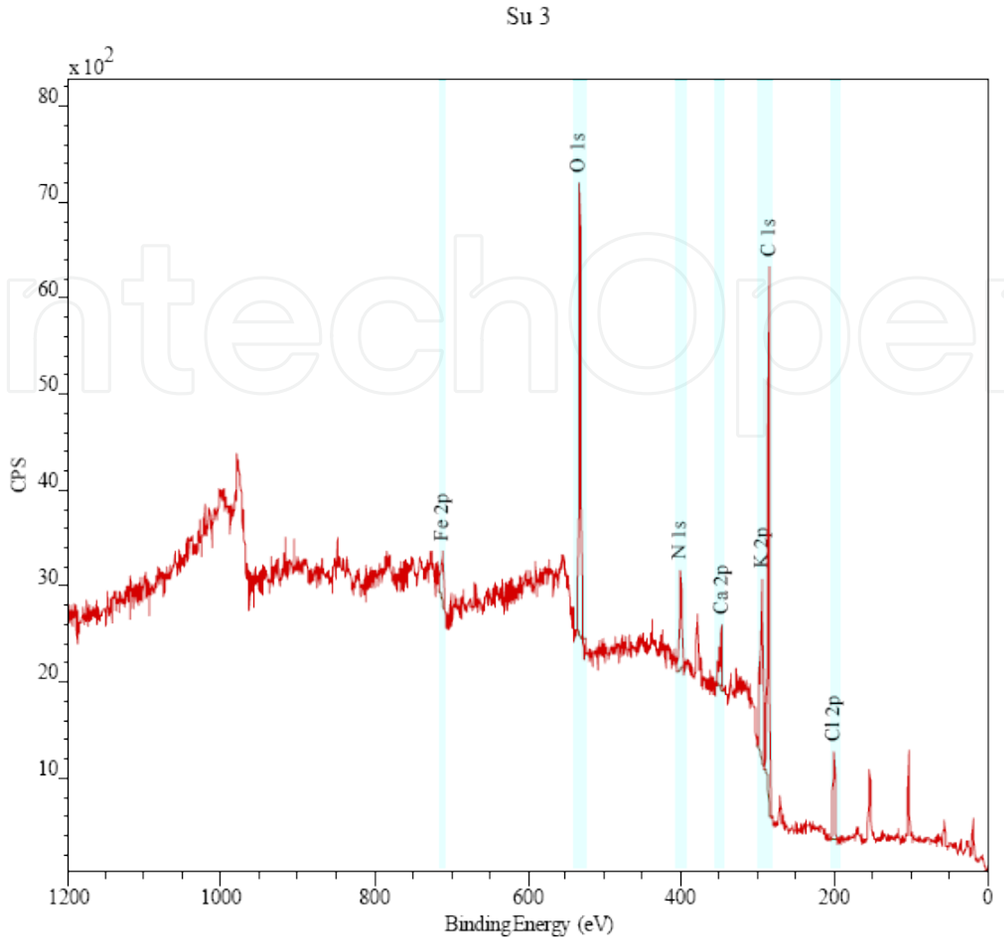

Figure 17. XPS measurement of PPy(MoO_4) on mild steel after delamination in 0.1 M $(Bu)_4NCl$ [44]

The release of molybdate in delamination process is confirmed by the XPS experiment of PPy(MoO_4)/mild steel in 0.1 M $(Bu)_4NCl$ [34]. After delamination, the PPy film was peeled off and molybdate was detected by XPS in the film. No signals of molybdate were found, only iron was seen in the spectra. The presence of iron may come from the corrosion process. The molybdate has moved to the defect during the corrosion process. The same SKP experiment was repeated and the amount of molybdate within the PPy film was measured by XPS at the defect and at the interface polymer/metal. The result is presented in Figure 18.

It can be seen that there is a difference of the amount of molybdate at the defect and at the interface polymer/substrate. At the defect, molybdate anions are expelled from the polymer due to the reduction of PPy when the defect is connected with the substrate galvanically. The amount of molybdate is consumed to form the passive layer and to suppress the cathodic delamination. Nevertheless, the PPy film is still in the oxidised state in the undelaminated region of PPy (point 2, Figure 18). Molybdate anions still remain in the PPy film. This is the reason why the quantity of molybdate in the PPy film at the defect is smaller than at the interface where the PPy protects the metal.

http://dx.doi.org/10.5772/54573

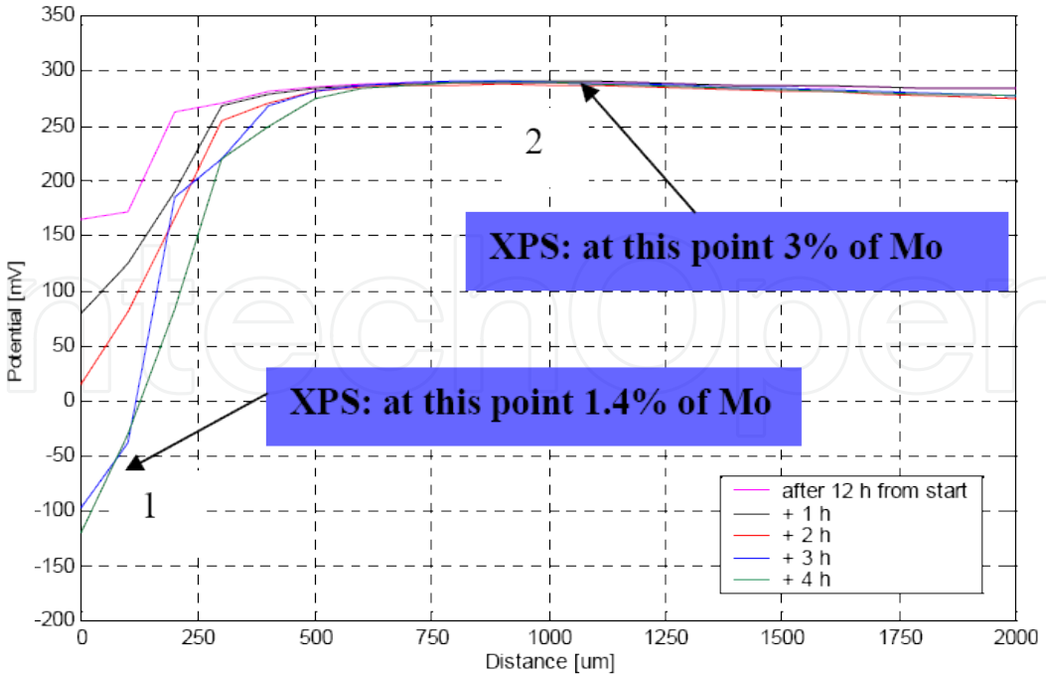

Figure 18. Quality of molybdate in the PPy film at the defect (1) and at the interface polymer/substrate (2) after delamination in 0.1 M $(Bu)_4NCl$ [44]

3.1.11. Raman spectroscopy of PPy(MoO_4)

During the corrosion process, PPy will be reduced because a galvanic cell is established between PPy and mild steel. Raman spectroscopy was used to characterise the state of PPy, oxidised or reduced.

PPy(MoO_4)/mild steel was prepared in aqueous solution of 0.1 M pyrrole + 0.01 M molybdate at 1.5 mA cm^{-2}. Three states of PPy (fully oxidised, partially reduced and totally reduced) were determined through the OCP obtained by dipping samples in 0.1 M NaCl. Raman spectra of these samples are shown in Figure 19.

Several bands are representative for the oxidised state. The band 1600 cm^{-1} belongs to the interring (C=C) of oxidized PPy (0.1 V). It shifts towards low wavenumbers in more negative potential (1597 cm^{-1} at –0.4 V and 1594 cm^{-1} at –0.6 V). The bands 1052 cm^{-1}, 1083 cm^{-1} are assigned to the C-H in plane deformation [50, 51]. They are also shifted to lower wavenumbers during the corrosion process. The Raman peaks of the dopant anion shift from 931 cm^{-1} to 920 cm^{-1} in the reduced state [52]. The PPy(MoO_4)/mild steel film is in the oxidised state while it protects mild steel substrate and is progressively changed to the reduced state during the protection progress.

The properties of PPy(MoO_4) can be summarised:

- PPy(MoO_4) films covered on mild steel have the effect of corrosion inhibition. The E_{corr} is in the passive range of potential in chloride solution. The potential shift is nearly 500 mV_{SCE} compared to bare mild steel. At the same time, i_{corr} decreases one order of magnitude when

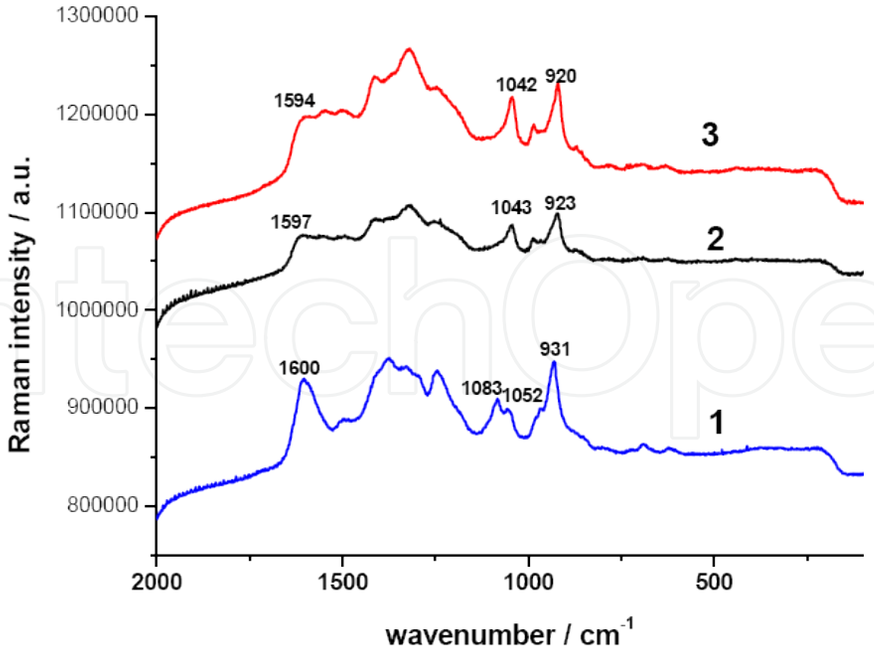

Figure 19. Raman spectra of PPy in different states: (1): complete oxidation (after formation), (2): partial reduction and (3): complete reduction

PPy(MoO_4) covers on mild steel. The protective efficiency is fairly high (about 98%), indicating a good property of PPy(MoO_4) in corrosion protection for mild steel.

- The self-healing effect of PPy(MoO_4) film can be observed by OCP measurement. In contrast, PPy(PF_6) cannot prevent corrosion of mild steel even with no defect. Molybdate in corrosion protection of mild steel is acting as anodic inhibitor.
- The release of the molybdate is necessary for self-healing of defect by PPy. The reduction of the PPy film during the corrosion process is the driving-force to release inhibitor anions. Raman experiments show that PPy changes from the oxidised state to the reduced state during the corrosion process. This observation is reported elsewhere [50, 53]. XPS results confirm this observation.
- The EQCM and EIS results in aqueous solution indicate that the reduction of PPy(MoO_4) is accompanied by a mixed anion/cation transport and by water uptake. However, it is possible to show that the medium size molybdate anion can be released from the film to improve the protective properties of PPy film deposited on mild steel.
- The Scanning Kelvinprobe experiments of PPy(MoO_4) film show that the release of molybdate can be found when the film is reduced in a large size cation solution. The delamination can be stopped. On the contrary, the delamination of PPy(MoO_4) film is fast in a small cation solution. The incorporation of cations is predominant. Therefore, the delamination cannot be hindered [34].
- The release behaviour of molybdate from the PPy film depends much on the size and mobility of cations in the electrolyte.

http://dx.doi.org/10.5772/54573

3.2. Epoxy coatings containing molybdate anions doped polypyrrole/montmorillonite nanocomposites

3.2.1. SEM images

Figure 20 shows SEM micrographs of PPy (a), MMT (b) and PPy(MoO_4)/MMT nanocomposite (c). As shown in Figure 20, PPy is black powder (Figure 20a) and MMT consists of platelet particles accumulating each other and as crystals (Figure 20b). Compared with MMT (Figure 20b), the hackly surface of PPy(MoO_4)/MMT nanocomposite can be seen due to the deposition of the PPy onto the layer surface of MMT (Figure 20c). At high magnification, it is easier to see the flaky structure of MMT (Figure 20c). One can observe (as shown in Figure 20c at the tip of the arrow) the antenna-like PPy ''stretching out'' from the layer surface of MMT.

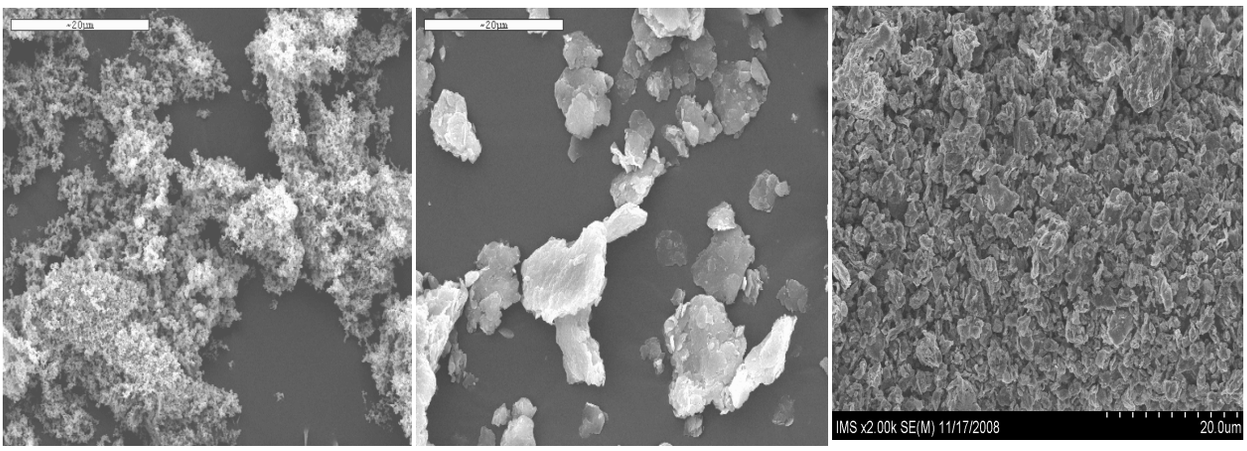

(a) (b) (c)

Figure 20. SEM images of PPy (a), MMT (b) and PPy/MMT nanocomposite (c)

3.2.2. XRD patterns

The XRD patterns of the materials before and after polymerization are shown in Figure 21. At first, Na^+-MMT was mechanically stirred for 30 min as reference. However, there are no changes in the XRD patterns of MMT before and after stirring. Therefore, the stirring does not affect the crystallinity of the MMT itself. The diffraction peak of Na^+-MMT was observed at $2\theta = 7.0°$, therefore, the basal spacing of Na^+-MMT was 1.22 nm (Fig. 21a). The intercalation of pyrrole monomers and dopant into MMT is shown in Figure 21b. The basal spacing increased from 1.22 nm to 1.58 nm ($2\theta = 5.8°$), indicating the expansion of the interlayer space (d-expansion) by 0.36 nm; and the successful intercalation by the mechanical intercalation method. The diffraction peaks of the products after polymerization were shifted to a higher angle than those before polymerization as shown in Figure 21c, indicating the synthesis of PPy in the clay layers. As a result, the the basal spacing of monomer-absorbed MMT changed from 1.58 nm to 1.42 nm ($2\theta = 6.0°$). They are in the agreement with other publications [54].

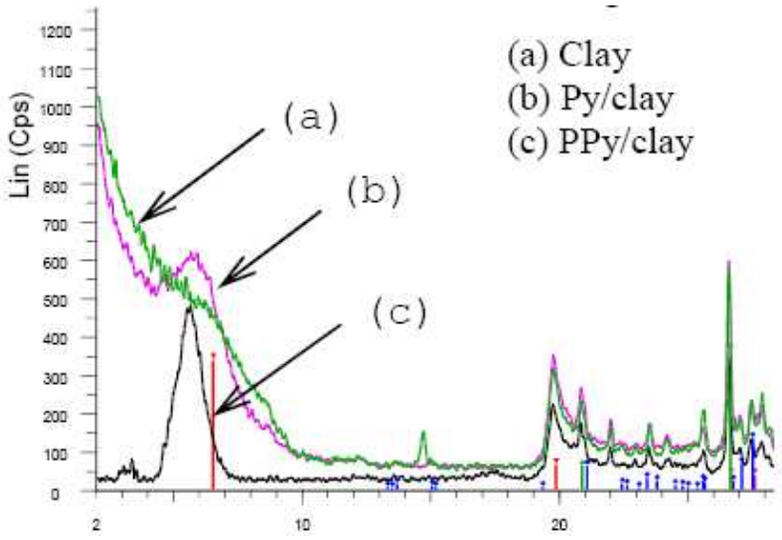

Figure 21. XRD patterns of MMT, monomer-absorbed MMT and PPy/MMT nanocomposites

3.2.3. Raman spectra

Figure 22 presents the Raman spectrum of PPy/MMT nanocomposite measured at 514 nm with 1 mW laser power. Table 1 gives the assignments of some Raman bands and compares the frequencies of the various vibration modes collected on the PPy/Ag spectra and with those theoretically calculated by Faulques *et al.* [55]. According to the theoretical values reported by Faulques et al. [55], the vibration frequency of the C=C double-bond of the PPy in the oxidized form (at 1593 cm^{-1}) is greater than that in the reduced form (Table 1). This evedence shows that molipdate anion was doped into PPy.

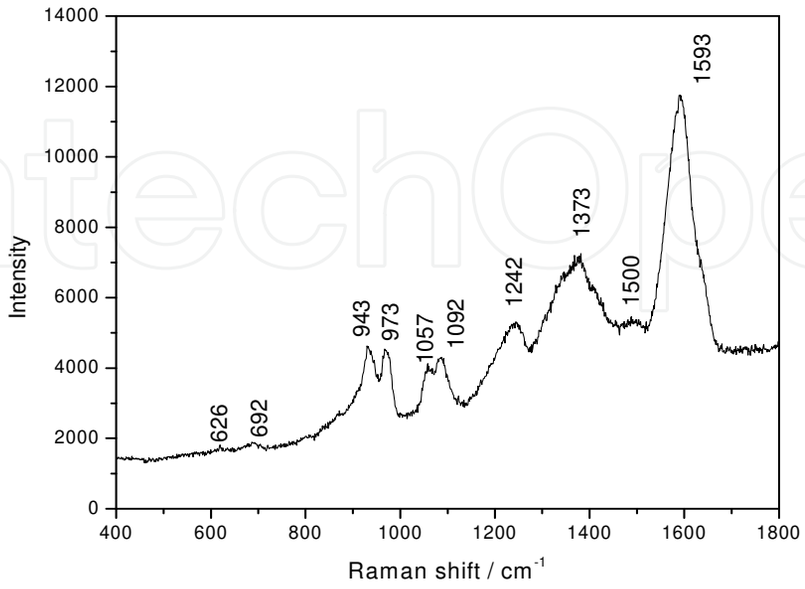

Figure 22. Raman spectrum of PPy(MoO_4)/MMT nanocomposite

Wavenumber (cm^{-1})			Assignment
Theoretical calculation [55] (oxidized PPy)	**PPy on Ag [56] (oxidized PPy)**	**PPy(MoO_4)/MMT (oxidized PPy)**	
1676.6	1584	1593	C=C ring stretching
1524.4	1414	1500	C-N stretching
1307.2	1327	1373	
-	1258	1242	
1049.4	1046	1057; 1092	C-H in plane deformation
955.8	989	973	C-H stretching
-	938	943	

Table 1. PPy/MMT nanocomposites and their components

3.2.4. EDX spectra

In order to determine the presence of molipdate anion in the synthetic nanocomposites EDX spectra were used. The EDX result of C6 is presented in Figure 23. The amount of element Mo in the nanocomposite PPy/MMT nanocomposite is 5,55%.

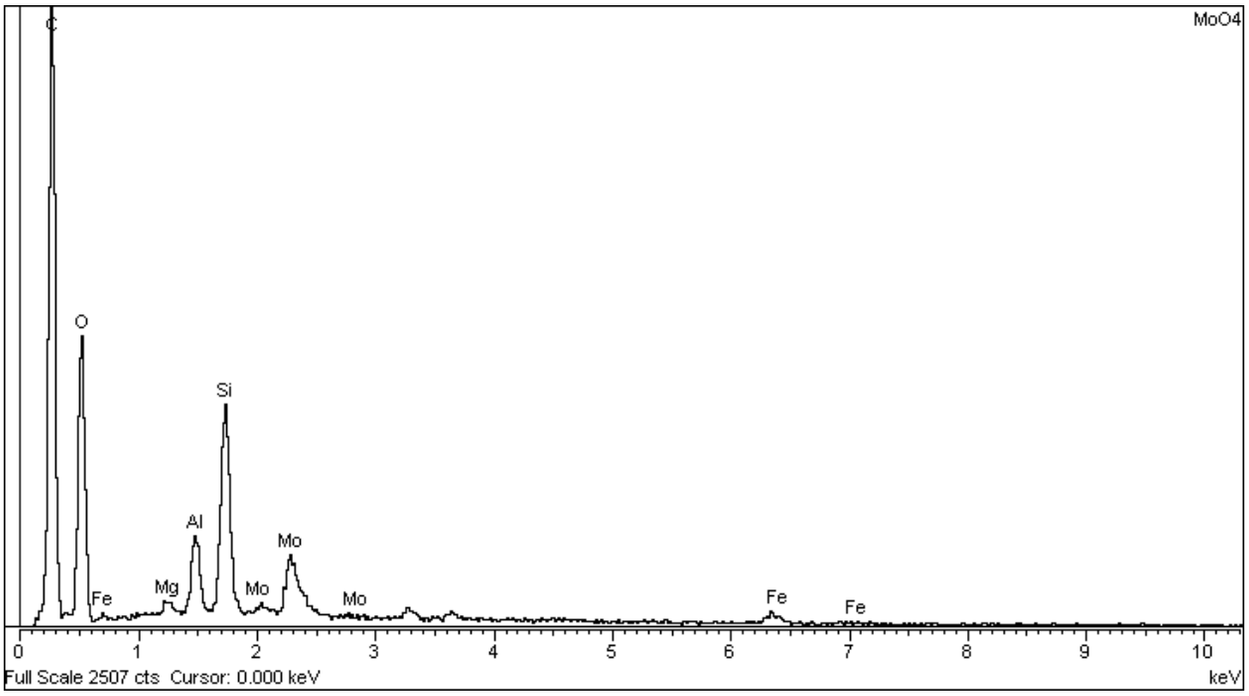

Figure 23. EDX spectra of PPy(MoO_4)/MMT nanocomposites

As seen in Figure 23 and Table 2, the amont of element Mo is 2.93% weight. It means that Na_2MoO_4 occupied 6.29% weight. In addition, the presence of other elements Si, Al, Mg, Fe, O in MMT and C in PPy component were presented in Fugure 23. Other peaks corresponding to hydrogen and nitrogen did not disappeared in EDX spectra.

Element	% Weight	% Element
C	54,53	64,15
O	37,07	32,74
Mg	0,27	0,16
Al	1,39	0,73
Si	3,33	1,68
Fe	0,46	0,12
Mo	2,93	0,43

Table 2. Amount of elements in PPy(MoO_4)/MMT nanocomposites

3.2.5. Thermal analyses

Thermal analyses of PPy(MoO_4)/MMT nanocomposites have been carried out. Figure 24 shows the thermal analyses curves of PPy(MoO_4)/MMT nanocomposites. Under 120^{0}C, the weight reduce origined from water inside samples. The strong reduce in this temperature range can be explained by the hydrophilic property of MMT and the oxidized state of PPy. It is also the source of the wide band between 4000 and 2500 cm^{-1} in the IR spectra. In the range of 120-330^{0}C, the weight reduces are very small, corresponding to the decomposition of redundant monomers, oligomers. At higher temparature (300-700^{0}C), the change of weight is attributed to the decomposition of the oxidized PPy. From Figure 24, the amounts of PPy in the PPy(MoO_4)/MMT nanocomposites are approximately calculated to be 16%.

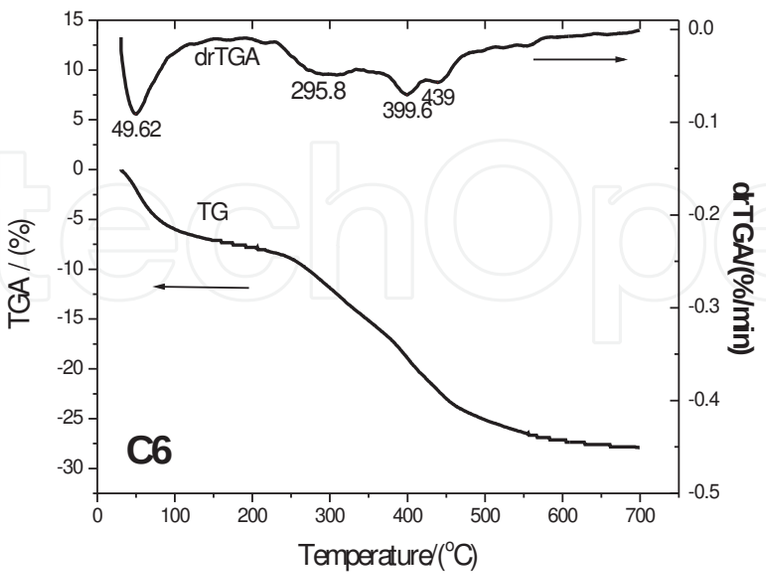

Figure 24. TGA curves and PPy(MoO_4)/MMT nanocomposite

http://dx.doi.org/10.5772/54573

3.2.6. Tests of corrosion protection

Figure 25 shows the OCP-time curves of steels covered by epoxy coatings contaning $PPy(MoO_4)$/MMT nanocomposite. It shows that the OPC of steel covered by epoxy was corroded after 2 weeks of immersion in NaCl solution. The OCP of the steel covered by epoxy coatings $PPy(MoO_4)$/MMT nanocomposite shows more possitive. Firstly the OCP of these samples gradually decreased and then increased (Figure 25). The reduction of OCP could be explained by the penetration of the corrosion medium. These results are in good agreement with that preasented in Figure 12. However, the OCP of these samples then incresed. These results shows the same phenomena of the sample $PPy(MoO_4)$/mild steel presented in Figure 11. When epoxy coating containing 2% $PPy(MoO_4)$/MMT, the OCP moved to anodic region from 7th day to 21st day and then keft plateau untill 42nd day. After that the OCP of A3 reduced to the value of -0.389VSCE on 56th day. In the case of epoxy containing 3% $PPy(MoO_4)$/MMT (sample A3), the OCP moved to anodic region from 7th to 28th day and keft plateu untill 42th day. On the 56th day, the OCP approached the value of -0.296V_{SCE}. When epoxy coating containing 4% $PPy(MoO_4)$/MMT, the OCP of the sample keft the constant value in the first week showing that the barier role of coating containing MMT. Then the OCP moved ossitively from 21st day to 28th day. This region could be explained by the by the penetration of the corrosion medium as weel as the situation of samples A2 and A3. After 42nd day, the OCP of sample A1 increased to -0.0087VSCE and keft plateau. This reason could be explained by the role of molybdate inhibitor anions. These rerults are in good agreement with that of $PPy(MoO_4)$/mild steel presented in section 3.1.

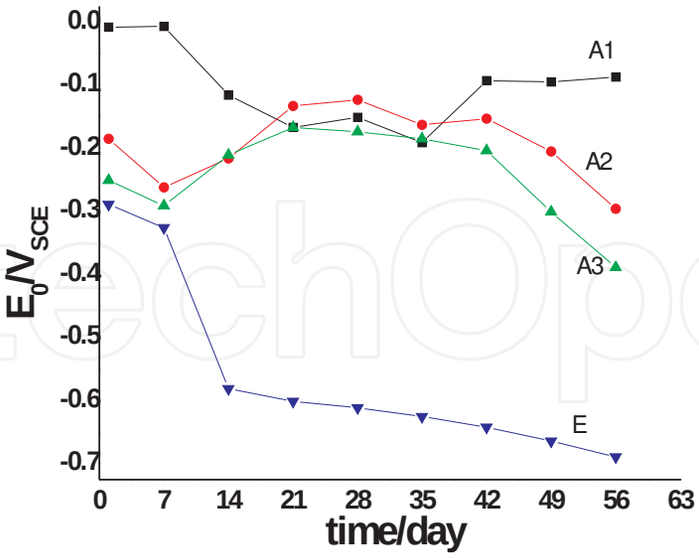

(A1: Epoxy containing 4% $PPy(MoO_4)$/MMT ; A2: Epoxy containing 3% $PPy(MoO_4)$/MMT ; A3: Epoxy containing 2% $PPy(MoO_4)$/MMT ; E: epoxy)

Figure 25. OCP-time curves of steel samples coverd epoxy coatings

In comparision with epoxy coating (sample E), all three epoxy coatings containing PPy(MoO_4)/MMT could prevent mild steel from corrosion (Figure 25).

Figure 26 shows the impedance – time curves at 1Hz of steels covered by epoxy coatings containing. At low frequency (1 Hz) the impedance of the system equals to the value of resistance of epoxy coating (Figure 3). Generally, the imdepance of epoxy coatings gradually reduced during time of immersion. These results could be explained by the penetration of the corrosion medium. Epoxy coating had lowest impedance because of no nanocomposites inside. The samples of A2 and A3 had the impedances of around 10^6 Ω and it was stable throughout experiments. The sample A4 epoxy coating containing 4% PPy(MoO_4)/MMT had highest impedance value at 1 Hz. It even increased after the 56th day (Figure 26). This reason could be explained by the role of molydate dopants.

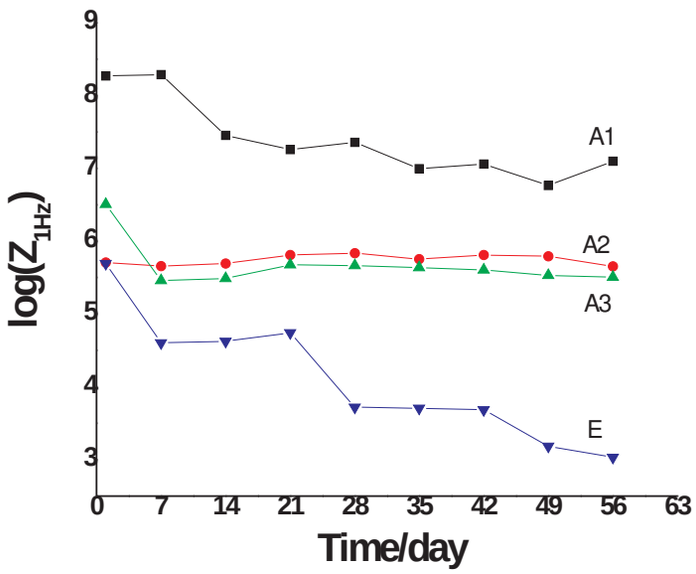

(A1: Epoxy containing 4% PPy(MoO_4)/MMT ; A2: Epoxy containing 3% PPy(MoO_4)/MMT ; A3: Epoxy containing 2% PPy(MoO_4)/MMT ; E: epoxy)

Figure 26. Impedance – time curves of steel samples coverd epoxy coatings

4. Conclusion

Inhibitors used as dopant anions in polymer films are responsible for the anticorrosion behaviour of PPy. The PPy film can work as self-repairing for small defects of the film. Molybdate was built-in into the film as dopant anion. The results of XPS revealed that molybdate exist in two types: $[MoO_4]^{2-}$ (62%) and $[Mo_7O_{24}]^{6-}$ (28%). The film was conductive, homogenous, and compact. Cyclic voltammograms have shown that the film was active. By scanning the potential, the Ppy film changed from the oxidised to the reduced state and at the

http://dx.doi.org/10.5772/54573

same time the anions were released from the polymer. To support this observation, Electrochemical Impedance Spectroscopy (EIS), Electrochemical Quartz Crystal Microbalance (EQCM) and Raman Spectroscopy were used. EIS has indicated the change of the resistance R_{PM} and the capacitance C_{PM} of the PPy film during reduction. EQCM has shown: the mass of the Ppy film decreased in the cathodic region and increased in the anodic region. The anion flux was also observed in Scanning Kelvinprobe (SKP) and X-ray Photoelectron Spectroscopy (XPS) experiments. The release of anion is one of the important factors of the corrosion protection property of the PPy film. However, the release behaviour of molybdate anions depends much on the size of cations in the electrolyte. At negative potentials, the incorporation of cations is predominant. Probably, molybdate is a medium size anion and not mobile enough to compete with the cations in the electrolyte for the moving in or out of the PPy film.

It should be also noted that PPy(MoO_4) can be electrodeposited on mild steel in a one-step process. No induction period was observed during polymerisation. PPy(MoO_4) shifted the corrosion potential of mild steel into the passive range. The corrosion current decreased simultaneously. The role of molybdate in corrosion protection was also investigated for Ppy films with small defects. The Open Circuit Potential (OCP) showed the fluctuations around -0.2 V_{SCE}. It means that the defect was passivated / repassivated continuously for 4 hours. It was assumed that molybdate was released from Ppy, move to the defect and act as corrosion inhibitor by forming a complex with iron ion.

The application of PPy(MoO_4)/MMT nanocomposites in corrosion protection for mild steel was also investigated in this work. Mixture of core-shell particles with a polymer was used as primer coatings. The positive effect on the corrosion protection of the coating was illustrated by the increase of the coating resistance and the stabilisation of the film capacitance during immersion in corrosive medium. These rerults show the promissing application potential to exchange the paints containing toxic cromate.

Author details

Le Minh Duc[1] and Vu Quoc Trung[2*]

*Address all correspondence to: vuquoctrungvn@netnam.vn

1 Faculty of Chemical Engineering, Danang University of Technology, Danang, Vietnam

2 Faculty of Chemistry, Hanoi National University of Education, Hanoi, Vietnam

References

[1] C. M. A. Brett, A. M. O. Brett, Electrochemistry: Principles, Methods and Application, 1993.

[2] R. W. Revie, Uhlig's Corrosion Handbook, John Wiley & Sons Inc, 2000.

[3] G.G. Wallace, G.M. Spinks, L.A.P. Kane-Maguire, P.R. Teasdale, Conductive Electroactive Polymers: Intelligent Materials Systems, CRC press, New York, 2003.

[4] W.K. Lu, R.L. Elsenbaumer, in: L. Rupprecht (Ed.), Conducting Polymers and Plastics in Industrial Applications, SPE, Norwich, NY, 1999, 195.

[5] N. Ahmad, A.G. MacDiarmid, Synth. Met., 78 (1996), 103.

[6] T. Schauer, A. Joos, L. Dulog, C.D. Eisenbach, Prog. Org. Coat., 33 (1998), 20.

[7] R.N. Rothon, Adv. Polym. Sci., 139 (1999), 67.

[8] A.M. Thayer, Chem. Eng. News, 81 (35) (2003), 15.

[9] N. V. Krstajic, B. N. Grgur, S. M. Jovanovic, V. Vojnovic, Electrochimica Acta, 42 (1997), 1685.

[10] Jude O. Iroh, W. Su, Electrochimica Acta, 46 (2000), 15.

[11] Michael Rohwerder, Adam Michalik, Electrochimica Acta, 53 (2007) 1300–1313

[12] G. Mengoli, M.T. Munari, P. Bianco, M.M. Musiani, J. Appl. Polym. Sci., 26 (12) (1981), 4247.

[13] D.W. Deberry, J. Electrochem. Soc., 132 (5) (1985), 1022.

[14] B. Wessling, Mater. Corros., 47 (1996), 439.

[15] J. Reut, A. O° pik, K. Idla, Synth. Met., 102 (1999), 1392.

[16] T.D. Nguyen, M. Keddam, H. Takenouti, Electrochem. Solid-State Lett., 6 (2003), B25.

[17] M. Rohwerdera, Le Minh Duc, A. Michalika, Electrochimica Acta, 54 (2009), 6075.

[18] G. Williams, H.N. McMurray, Electrochem. Solid State Lett., 8 (2005), B42.

[19] Victoria Johnston Gelling, Michelle M. Wiest, Dennis E. Tallman, Gordon P. Bierwagen, Gordon G. Wallace, Prog. in Org. Coatings, Volume, 43 (1-3) (2001), 149.

[20] H. N. T. Le, B. Garcia, C. Deslouis, Q. L. Xuan, J. of App. Electrochem., 32 (2002) 105.

[21] N. T. H. Le, B. Garcia, A.Pailleret, C. Deslouis, Electrochimica Acta 50, (2005), 1747.

[22] A. Michalik, M. Rohwerder, Z. Phys. Chem., 219 (2005), 1547.

[23] G. Paliwoda-Porebska, M. Stratmann, M. Rohwerder, U. Rammelt, L. Minh Duc, W. Plieth, J. Solid State Electrochem., 10 (2006), 730.

[24] G. Paliwoda, M. Stratmann, M. Rohwerder, K. Potje-Kamloth, Y. Lu, A.Z. Pich, H.-J. Adler, Corros. Sci., 47 (2005), 3216.

[25] F. Beck, U. Barsch, R. Michaelis, J. of Electroanalytical Chemistry, 351 (1993), 169.

[26] U. Rammelt, P. T. Nguyen, W. Plieth, Electrochimica Acta, 48 (2003), 1257.

[27] U. Rammelt, P. T. Nguyen, W. Plieth, Electrochimica Acta, 46 (2001), 4251.

[28] M. Kendig, M. Hon, L. Warren, Progress in Organic Coating, 47 (2003), 183.

[29] Pierre R. Roberge, Handbook of corrosion engineering, McGraw-Hill, 2000.

[30] G. M. Spinks, A. J. Dominis, G. G. Wallace, D. E. Tallman, J. of Solid State Electrochem., 6 (2002), 85.

[31] P. J. Kinlen, D. C. Silverman, C. R. Jeffreys, Synthetic Metals, 85 (1997), 1327.

[32] J. He, V. J. Gelling, D. E. Tallman, G. P. Bierwagen, G. G. Wallace, J. of Electrochem. Soc., 147 (2000), 3667.

[33] P. J. Kinlen, V. Menon, Y. Ding, J. of Electrochem. Soc., 146 (1999), 3690.

[34] G. Paliwoda-Porebska, M. Rohwerder, M. Stratmann, U. Rammelt, L. M. Duc, W. Plieth. J. of Solid State of Electrochem., 10 (2006), 730.

[35] U. Rammelt, L. M. Duc, W. Plieth, J. of Appl. Electrochem., 35 (2005),1225.

[36] W. Plieth, A. Bund, U. Rammelt, S. Neudeck, L.M.Duc, Electrochimica Acta, 2005.

[37] Yongqin Han, Polymer composite, 30 (1) (2009), 66.

[38] S.H. Hong, B.H. Kim, J. Joo, J.W. Kim, Hyung J. Choi, Current Applied Physics, 1 (6), (2001), 447.

[39] S. U. Rahman, M. S. Ba-Shamakh, Synthtic Metals, 140 (2004), 207.

[40] V. S. Sastri, Corrosion inhibitor- Principles and Applications, Wiley, 1998.

[41] G. Reinhard, M. Radtke, U. Rammelt, Corrosion Science, 33 (1992), 307.

[42] F. Beck, R. Michaelis, F. Schloten, B. Zinger, Electrochimica Acta, 39 (1994), 229.

[43] W. Su, Jude O. Iroh, Electrochimica Acta, 44 (1999), 2173.

[44] G.Paliwoda-Porebska, PhDThesis, Bochum Universtity, Germany, 2005.

[45] E. Almeida, T. C. Diamantino, M. O. Figueiredo, C. Sa, Surface and Coatings Tech., 106 (1998), 8.

[46] T. V. Vernitskaya, O. N. Efimov, A. B. Gavrilov, Russ. J. of Electrochem., 30 (1994), 1022.

[47] M.C. Bernard, S. Joiret, A. Hugo-Le Goff, P.V. Phong, J. of Electrochem. Soc., 148 (2001), B12.

[48] K. Aramaki, Corrosion science, 42 (2000), 1975.

[49] A. Leng, H. Streckel, M. Stratmann, Corrosion Science, 41 (1999), 547.

[50] H. N. T. Le, M. C. Bernard, B. G. Renaud, C. Deslouis, Synthetic Metals, 140 (2004), 287.

[51] Y. Chuan Liu, B. J. Hwang, Synthetic Metals, 113 (2000), 203.

[52] F. Chen, G. Shi, M. Fu, L. Qu, X. Hong, Synthetic Metals, 132 (2003), 125.

[53] T. D. Nguyen, T. Anh Nguyen, M. C. Pham, Electroanalytical Chemistry, 572 (2004), 225.

[54] S. Yoshimoto, F. Ohashi, Y. Ohnishi and T. Nonami, Chem. Commun., 17, (2004), 1924.

[55] A. Faulques, W. Wallnoefer, H. Kuzmany, J. Chem. Phys., 90 (12), (1989), 7585.

[56] M. Bazzaoui, E. A. Bazzaoui, L. Martins and J. I. Martins, Synthetic Metals, 128 (1), (2002), 103.